Published in final edited form as:
Circulation. 2009 September 15; 120(11 Suppl): S112–S119. doi:10.1161/CIRCULATIONAHA.108.844159.

Significant Changes in Mitral Valve Leaflet Matrix Composition and Turnover With Tachycardia-Induced Cardiomyopathy

Elizabeth H. Stephens, BS, **Tomasz A. Timek, MD**, **George T. Daughters, MD**, **Joyce J. Kuo, BS**, **Aaron M. Patton, BS**, **L. Scott Baggett, PhD**, **Neil B. Ingels, PhD**, **D. Craig Miller, MD**, and **K. Jane Grande-Allen, PhD**
From Department of Bioengineering (E.H.S., J.J.K., A.M.P., K.J.G.-A.) and Department of Statistics (L.S.B.), Rice University, Houston, Tex; Department of Cardiothoracic Surgery (T.A.T., G.T.D., N.B.I., D.C.M.), Stanford University School of Medicine, Stanford, Calif; Department of Cardiovascular Physiology and Biophysics (N.B.I., D.C.M.), Research Institute, Palo Alto Medical Foundation, Palo Alto, Calif.

Abstract

Background——Dilated cardiomyopathy (DCM) involves significant remodeling of the left ventricular–mitral valve (MV) complex, but little is known regarding the remodeling of the mitral leaflets. The aim of this study was to assess changes in matrix composition and turnover in MV leaflets with DCM.

Methods and Results——Radiopaque markers were implanted in 24 sheep to delineate the MV; 10 sheep underwent tachycardia-induced cardiomyopathy (TIC), whereas 14 sheep remained as controls. Biplane videofluoroscopy was performed before and after TIC. Immunohistochemistry was performed on leaflet cross-sections taken from the septal, lateral, anterior, and posterior commissures attachment segments. Staining intensity was quantified within each attachment segment and leaflet region (basal, mid-leaflet, and free edge). Mitral regurgitation increased from 0.2±0.4 before TIC to 2.2±0.9 after TIC (P<0.0002). TIC leaflets demonstrated significant remodeling compared to controls, including greater cell density and loss of leaflet layered structure (all P<0.05). Collagen and elastic fiber turnover was greater in TIC, as was the myofibroblast phenotype (all P<0.05). Compositional differences between TIC and control leaflets were heterogeneous by annular segment and leaflet region, and related to regional changes in leaflet segment length with TIC.

Conclusions—This study shows that the MV leaflets are significantly remodeled in DCM with changes in leaflet composition, structure, and valve cell phenotype. Understanding how alterations in leaflet mechanics, such as those induced by DCM, drive cell-mediated remodeling of the extracellular matrix will be important in developing future treatment strategies.

Keywords

cardiomyopathy; collagen; immunohistochemistry; metalloproteinases; mitral valve

Although numerous studies have demonstrated the importance of the mitral valve (MV) annulus in proper MV function and in the development of dilated cardiomyopathy (DCM),[1,2] the MV leaflets have been largely considered bystanders in DCM. A recent study, however,

Correspondence to K. Jane Grande-Allen, PhD, Bioengineering, Rice University, PO Box 1892-MS142, Houston, TX 77251-1892. grande@rice.edu.

Presented in part at American Heart Association Scientific Sessions 2008, November 8–12, 2008, New Orleans, La.

Disclosures
D. Craig Miller is a consultant for Medtronic Heart Valve Division, Inc.

demonstrated changes in the MV leaflet geometry after tachycardia-induced cardiomyopathy (TIC) that were not solely attributable to annular dilation.3 One potential explanation for these changes is that TIC altered the mechanical loads applied to the valve leaflets, which stimulated the valvular interstitial cells (VIC) to alter their phenotype and normal patterns of extracellular matrix synthesis and remodeling.4 Changes in the composition and arrangement of the extracellular matrix in the valve leaflets would, in turn, influence their structure and material behavior. Therefore, the objective of this study was to characterize the changes in matrix composition, matrix turnover, and VIC phenotype that occurred in mitral leaflets as a result of TIC and to relate these to leaflet segment length changes. This information should give insight into the pathogenesis of DCM and may help to improve current reparative techniques.

Materials and Methods

All animals received humane care in accordance with the guidelines of the US Department of Health and Human Services (NIH Publication 85-23, Revised 1985). The use of animals in this study was approved by the Stanford Medical Center Laboratory Research Animal Review Committee.

Animal Protocol

Radiopaque markers were implanted in 24 sheep (Robert McGrew, Dixon, Calif) delineate the leaflet and annulus of 4 MV segments (Figure 1): septal (SEPT), lateral (LAT), and anterior commissure (ANT-C), and posterior commissure (POST-C). The marker implantation procedure has been described in detail previously.5 Ten sheep underwent a rapid-pacing protocol (TIC) for an average of 15±6 days,5 whereas 14 sheep used for an acute hemodynamic study were used as histological controls (CTRL). Biplane video fluoroscopy was performed in CTRL and both before and after pacing in TIC animals. TIC-induced changes in maximum and minimum septal and lateral leaflet lengths throughout the cardiac cycle were measured for basal leaflet (BL) and mid-leaflet (ML) regions (Figure 1). The septal-lateral diameter was measured as the maximum distance between the mid-septal and mid-lateral annular markers throughout the cardiac cycle, whereas the commissure–commissure diameter was measured as the maximum distance between the 2 commissural annular markers throughout the cardiac cycle. Although animals were not randomly assigned to groups, all animals (CTRL and pre-TIC) displayed hemodynamic parameters in the normal range and showed comparable percentage changes in annular or leaflet segment distances throughout the cardiac cycle. Mitral regurgitation was graded on a scale of 0 to 4 based on color Doppler regurgitant jet extent and width,6 as previously described.5 Left ventricular (LV) end-diastolic volume (EDV), and end-systolic volume (ESV) were calculated using a space-filling analysis of epicardial markers, as described.5 Ejection fraction (EF) was calculated as the difference between EDV and ESV, divided by EDV. These calculated EF values consistently underestimate the true EF because the calculated EDV includes LV myocardial mass, but EF calculations were only used to assess potential correlations between LV remodeling and leaflet changes among the TIC animals. At the end of the study, the hearts were then harvested and stored in formalin. Control animals were used for histological comparison only, whereas hemodynamic and leaflet segment length analyses compared pre-TIC and TIC data.

Histology and Immunohistochemistry

Cross-sections 3 to 5 mm in width were cut from insertion region (including associated myocardium) to free edge (Figure 2), embedded in paraffin, and sectioned to a thickness of 5 μm. Sections were stained with Movat pentachrome to demonstrate the layered structure of the leaflet. Immunohistochemistry was performed for a number of extracellular matrix components and turnover proteins (Table 1). For each segment (LAT, SEPT, ANT-C, POST-C; Figure 1), staining intensity was quantified within each leaflet region (BL, ML, and free edge) and

histological layer (fibrosa, atrialis, spongiosa [spongiosa only in ML]) using ImageJ software (NIH, Bethesda, Md). The free edge was considered a single layer. Cell density was assessed by counting nuclei within a defined area of the BL and ML fibrosa, as well as the free edge. Semiquantitative grading was performed on blinded sections using a predetermined grading rubric ranging from 0 (minimum) to 4 (maximum) for delineation between leaflet layers and diffusion of Movat-stained collagen beyond the fibrosa. Percentage differences in histological and immunohistochemistry parameters between TIC and CTRL were calculated by comparing each TIC value to the average CTRL value for a given parameter.

Statistical Analysis

SigmaStat (SPSS, Chicago, III) was used for multivariate ANOVA with significance set at 0.05. Non-normally distributed data sets underwent rank transformation before the ANOVA. In 1 case, $P<0.05$ on the ANOVA before the data were rank-transformed, but $P>0.05$ in the ANOVA after the data were rank-transformed. In this case the P value from the ANOVA before the data were rank-transformed is given followed by an "R." Paired t tests were used for the statistical comparison of pre-TIC and post-TIC hemodynamics. Correlations between staining intensities of different proteins within individual leaflet layers, regions, and segments (to assess colocalization of cell activation and matrix remodeling) were calculated using a Pearson rank order test for normally distributed data and Spearman rank order correlation test for non-normally distributed data. Correlations between protein intensities and TIC-induced changes in segment lengths, EDV, ESV, and EF (to relate compositional changes, altered strain, and LV remodeling within individual animals) were similarly determined. For correlations between intensities of different proteins $P\leq0.015$ was considered a trend and $P\leq0.00625$ was considered significant (because the intensities of 8 proteins were being compared); for correlations between intensities of proteins and TIC-induced segment length and EDV, ESV, EF changes, each protein was considered individually; therefore, $P\leq0.05$ was considered significant. Data are presented as mean and SD, unless otherwise noted. Percentages for IHC are presented as mean and SEM because of the multiple segments, layers, or regions involved in the statistical tests.

Statement of Responsibility

The authors had full access to the data and take responsibility for its integrity. All authors have read and agree to the manuscript as written.

Results

Dynamic Leaflet Changes After the Development of Dilated Cardiomyopathy

Consistent with the development of DCM, the maximum annular septal-lateral diameter increased 24±9% ($P<0.0001$) in TIC compared to pre-TIC, the commissure–commissure diameter increased 9±4% ($P<0.001$), and mitral regurgitation increased from 0.2±0.4 to 2.2 ±0.9 (Figure 3; $P<0.0002$). Further characterization of annular and hemodynamic changes with TIC has been previously published.[3,5] Leaflet segment lengths increased with TIC compared to pre-TIC for both LAT and SEPT (Table 2; 8±12%; each $P<0.05$). In LAT and SEPT, the TIC-induced increase in the maximum ML length was greater than that of the BL (13±12% versus 5±10%; $P=0.018$), and the TIC-induced increase in the maximum ML length of LAT was greater than SEPT (14±5% versus 5±5%; $P=0.032$).

Structural Changes in TIC Leaflets

Compared with CTRL, SEPT and LAT of TIC showed greater cell density across all leaflet regions (57±17%; $P=0.05$; and 94±17%; $P<0.001$), as did ANT-C/POST-C (39±11%; $P=0.05$). TIC leaflets showed less delineation between valve layers compared to CTRL (Figure 4A,B;

−20±5%; *P*=0.014) with collagen more likely to be spread beyond the fibrosa layer (37±8%; *P*=0.002). There was also an increased incidence of muscle in TIC leaflets compared to CTRL (9 TIC versus 2 CTRL samples; Figure 4C).

Greater Collagen Turnover in TIC Leaflets

Collagen turnover was examined by staining for collagens I and III and matrix metalloproteinase (MMP)-13. MMP-13 in TIC ML was greater than in CTRL when all segments were considered (Figure 5; 15±3%; *P*=0.005), as well as in ANT-C individually (42 ±10%; *P*=0.012), whereas no significant differences were seen in BL. MMP-13 in the atrialis and fibrosa layers of TIC LAT was also greater than in CTRL (12±6%; *P*=0.002), whereas SEPT did not show such differences. Collagen I in TIC ML was greater than in CTRL when all segments were considered (Figure 6; 9±3%; *P*=0.036), as well as in ANT-C alone (32±8%; *P*=0.004), whereas no significant differences were seen in BL when all segments were assessed. Collagen I in LAT BL (24±7%; *P*=0.020), the atrialis and fibrosa layers of LAT (20±4%; *P*=0.002), and all regions of ANT-C (46±12%; each $P \leq 0.008$) was greater in TIC compared to CTRL. Collagen III in LAT BL (14±5%; *P*=0.035) and ANT-C fibrosa (32±7%; *P*=0.003) was greater in TIC compared to CTRL, but was less in SEPT across all regions (−15±6%; each $P \leq 0.009$). In fact, collagen III in SEPT ML atrialis negatively correlated with TIC-induced changes in SEPT ML maximum and minimum length ($r=-0.671$; *P*=0.021; and $r=-0.647$; *P*=0.029). Evidence for collagen turnover was further suggested by correlations between collagens I and III with MMP-13 in the ML of ANT-C and POST-C ($r=0.744$–0.779; each $P<0.015$). Lysyl oxidase, which is involved in both collagen and elastic fiber synthesis, was greater in TIC POST-C ML compared to CTRL (16±4%; *P*=0.012), whereas no significant differences were noted in any of the BL segments.

Greater Elastic Fiber Turnover in TIC Leaflets

Elastic fiber turnover was examined by staining for elastin and MMP-9, in addition to lysyl oxidase. In TIC, MMP-9 in ML of all segments was greater than CTRL (Figure 7; 11±3%; *P*=0.003), but no such differences were seen in BL. MMP-9 in LAT atrialis and fibrosa was also greater in TIC compared to CTRL (7±4%; *P*=0.015), whereas SEPT did not show such differences. Elastin in SEPT ML was greater in TIC (40±7%; $P<0.001$), whereas no significant differences were noted in BL. When examined by layers, the atrialis and fibrosa of both SEPT and LAT contained more elastin in TIC (atrialis: 28±9%, $P<0.001$; fibrosa: 25±4%, *P*=0.032R). This greater abundance of both elastin and MMP9 suggests elastic fiber remodeling, especially given that their degree of expression correlated with one another in certain leaflet regions (ie, LAT ML atrialis, $r=0.765$; $P<0.0025$). Expression of elastin correlated to changes in leaflet segment length. For example, elastin in SEPT ML fibrosa positively correlated with TIC-induced changes in SEPT minimum ML length ($r=0.683$; $P<0.007$).

Proteoglycans and Glycosaminoglycans in TIC Leaflets

In TIC, the glycosaminoglycan hyaluronan in LAT ML was less than in CTRL (−11±4%; *P*=0.021); no significant differences were noted in any BL segments or for SEPT. The abundance of hyaluronan in LAT BL atrialis negatively correlated with TIC-induced changes in maximum BL length ($r=-1.00$; *P*=0.017). Expression of the proteoglycans biglycan and decorin showed minimal changes with TIC.

Greater Valve Cell Activation in TIC Leaflets

Activation of VIC was assessed by staining for smooth muscle α-actin (SMaA) and nonmuscle myosin, proteins indicating the contractile, highly synthetic myofibroblast phenotype.[8] In ML, SMaA in TIC was greater than in CTRL for all segments except SEPT (Figure 8; 21±3%; each $P \leq 0.018$); no significant differences were evident in BL. SMaA in POST-C free edge in TIC

was also greater than in CTRL (28±6%; P=0.049). Nonmuscle myosin in ML was greater for TIC when all segments were considered (7±2%; P=0.046), as well as in POST-C individually (13±3%; P=0.032). Nonmuscle myosin in LAT BL (13±5%; P=0.049) was also greater in TIC.

Cell Activation and Correlations Between Proteins Within Leaflet Regions and Layers

There were numerous correlations between the phenotypic indicators of valve cell activation (Nonmuscle myosin, SMaA) and matrix degradation proteins (MMP-9, MMP-13), particularly in the spongiosa and fibrosa of the different segments (r=0.831–0.874; $P\leq$0.002), with strong correlation between SMaA and MMP-13 in BL fibrosa across segments (r=0.808; P<0.001).

Relationship of LV Remodeling to Observed Leaflet Changes

The degree of LV remodeling, as measured by percent changes in EDV, ESV, and EF with TIC, was often predictive of leaflet changes. For instance, decreases in EF with TIC were correlated with reductions in expression of collagen I in the atrialis and fibrosa layers of LAT ML (r=0.973; P<0.001) and greater expression of collagen III in ANT-C ML and BL (r= −0.765; P=0.0163). As EDV and ESV increased, SMaA and MMP-13 in the ML fibrosa of ANT-C were increased (SMaA: r=0.921–0.956, $P\leq$0.0261; MMP13: r=0.858–0.861, $P\leq$0.029). LV remodeling also was predictive of changes in leaflet structure. For example, diffusion of collagen in LAT increased with EDV (r=0.911; P=0.00115) and cell density in LAT ML increased with both EDV and ESV (r=0.834–0.835; $P\leq$0.0388). Different leaflets, however, responded in distinct ways to the LV remodeling; some changes in SEPT (ie, MMP-13 in ML fibrosa) were inversely related to EDV and ESV.

Discussion

TIC leaflets demonstrated significant remodeling compared to CTRL, including greater cell density, less delineation between leaflet layers, greater collagen and elastic fiber turnover, and evidence of valve cell activation. Compositional differences between TIC and CTRL leaflets were heterogeneous by annular segment and leaflet region with extracellular matrix changes generally greater in the ML than the basal leaflet, consistent with the magnitude of leaflet length changes in these regions. Greater expression of markers of cell activation in TIC suggests an increase in the myofibroblast population; these contractile and synthetic VIC may in part be responsible for these changes in leaflet segment length and composition with TIC. Statistical correlations provided the first in vivo demonstration to our knowledge of direct relationships between the degree of mechanical strain and the magnitudes of phenotypic changes in VIC and valve matrix within individual animals.

Changes in Matrix Composition Are Heterogeneous

TIC affected the leaflet regions heterogeneously, with greater compositional and leaflet length changes in the ML than in the BL region. Decreased coaptation could cause the distal ML and free edge to experience less of the compressive forces associated with coaptation, potentially increasing stresses in those regions and directly adjacent regions,[1] which could instigate larger compositional changes in the ML than the BL. Increased stress on valves[9] and valve cells[4] has been shown to cause increased matrix production and valve cell activation, as found in this study. Furthermore, with a decrease in the compressive forces associated with coaptation, leaflet segment lengths should increase, particularly in the distal leaflet, as noted in this study.

In terms of layers, changes in composition between TIC and CTRL largely consisted of changes in the atrialis and fibrosa layers. Both the atrialis and fibrosa normally contain significant amounts of collagen, and given our finding of increased collagen turnover, it is logical for changes in composition to be evident in these layers. Furthermore, leaflet length changes largely correlated with compositional changes in the atrialis and fibrosa, consistent with the

role these layers are thought to play in providing leaflet tensile strength.[10] It is interesting to note that significant changes in elastic fiber turnover were found in the fibrosa, a layer not dominated by elastic fiber content; these changes may have been induced by increased radial deformation.

The various segments also showed significant heterogeneity in response to TIC. Compared to CTRL, LAT showed changes in valve cell activation, matrix components, and matrix remodeling proteins, such as SMaA, collagen I, MMP-9, and MMP-13, as well as ML thickening, but SEPT did not show these changes. Greater TIC-related changes in matrix composition in LAT compared to SEPT are consistent with greater leaflet length changes in LAT. These results corroborate previous studies of both computational modeling and animal model experiments. Kunzelman et al,[1] in modeling the stresses of various portion of the MV after annular dilation, found that the increased stress was mostly on the lateral leaflet. Whereas changes in SEPT were less pronounced than in LAT, both the fluoroscopy and immunohistochemical results suggest that SEPT did remodel in TIC. Septal showed increased leaflet length, cell density, and elastin in TIC compared to CTRL. Interestingly, unlike the other segments, SEPT showed a decrease in collagen III. This unique remodeling pattern could imply a shift in the balance of mechanical loads between the various parts of the MV. In another recent study performed by this group, similar results of greater collagen and elastic fiber turnover were found in the septal leaflet when that leaflet was exposed to isolated regurgitation for 12 weeks.[11] Given the mitral regurgitation present in TIC and the results of this previous study, some of the changes observed in SEPT of TIC could be attributable to the regurgitation that is a part of DCM.

In terms of the commissural segments, TIC-induced changes in collagen turnover in the ANT-C resembled LAT with greater collagen I, collagen III, and MMP-13 compared to CTRL However, neither commissure displayed any alterations in elastic fiber turnover proteins (elastin, MMP-9, and lysyl oxidase), whereas both LAT and SEPT did. Although ANT-C and POST-C appeared to Show distinct responses to TIC, further work is needed to clarify the role of the commissural remodeling in TIC.

Influence of Mitral Regurgitation and LV Remodeling

Mitral regurgitation imposes altered hemodynamics on all of the mitral valve leaflets and commissures, including altered flow patterns,[12] in addition to the forces secondary to decreased or delayed coaptation;[1] all of which could have contributed to the changes observed in the TIC leaflets. Indeed, previous studies have documented increased collagen content in rat MV under acute increased LV pressure.[13] However, TIC animals displayed global LV[5,14] and even neurohormonal[15] changes in addition to mitral regurgitation, mimicking the clinical condition of DCM. Therefore, the leaflet changes observed with TIC are likely not solely attributable to mitral regurgitation, but could be secondary to altered forces imposed by changes in mitral annular shape and contractility,[5] or even circulating neurohormones as documented in TIC animals.[15]

The predictive relationships between LV remodeling and leaflet changes observed in this study highlight how DCM results in alterations in a variety of the normal array of forces that comprise the mechanical environment of the MV. These relationships confirm that the leaflets are integral to LV structure and function. It is also important to note that these predictive relationships were unique to the different leaflets, which is consistent with the heterogeneity of the MV leaflets in relationship to LV structure, function, and response to DCM.

Changes in Phenotype and Matrix Markers Implicate Role of Myofibroblasts

The correlations between amounts and locations of valve cell activation and matrix degradation proteins, along with previous studies demonstrating the capacity of these cells for matrix synthesis and remodeling capabilities,[8,16] provide strong evidence for the involvement of activated myofibroblasts in the matrix changes observed with TIC. These findings are consistent with the greater expression of myofibroblast markers in TIC leaflets and, more importantly, demonstrate direct relationships between magnitude of matrix remodeling, cell activation, and leaflet strain in individual animals. These results also strengthen evidence for the presumed role of VIC myofibroblasts in multiple valve diseases and remodeling processes.[16] Furthermore, considering the contractile properties of valvular myofibroblasts,[8] which have been shown to modulate leaflet stiffness,[4] these myofibroblast cells may be responsible in part for the heterogeneous TIC-induced changes in valve geometry and strain. We speculate that in diseases in which leaflet motion and composition are altered, the myofibroblast may be a target cell population for treatment strategies.

Implications for Human DCM

The results of this study corroborate findings in human DCM. Chaput et al[17] recently documented leaflet remodeling, namely increased leaflet area, in patients with functional mitral regurgitation, and Grande-Allen et al[18] reported increased DNA, collagen, and glycosaminoglycans in valves from heart failure patients compared to controls. Consistent with those previous findings, this study found greater cell density and collagen in TIC ovine leaflets compared to CTRL. The increase in MMP demonstrated in this study is also consistent with findings of greater expression of MMP in the ventricles of human patients with DCM.[19]

The compositional changes observed in this study could have functional consequences. The greater amount of collagen would be expected to make the leaflets more stiff, as observed in explanted DCM leaflets.[20] Computational studies have shown that such increased stiffness leads to delayed and incomplete coaptation and ultimately mitral regurgitation.[21] Computational modeling has also demonstrated that loss of the well-defined layered structure of the leaflets would increase leaflet bending stresses.[22] Greater elastic fiber turnover suggests less mature elastic fibers, which could lead to less leaflet recoil. Both the changes in stiffness and layered nature of the leaflet could worsen mitral regurgitation and lead to further adverse leaflet remodeling.[11] Indeed, although the study of functional mitral regurgitation by Chaput et al[17] did not examine leaflet composition, they found that remodeling of the leaflet anatomy, specifically the leaflet-to-closure area ratio, significantly correlated with mitral regurgitation severity, after adjusting for LV remodeling, function, and leaflet tethering. Their results are consistent with the speculation that the leaflet remodeling demonstrated in this study would lead to functional impairment. In the future, it will be important to demonstrate these proposed mechanisms for valve tissue dysfunction, perhaps using novel bioengineering approaches.

Limitations

One limitation in this study is the short time course. Clinically, DCM occurs over a period of years, whereas in this model the animals experienced DCM for only 15 days. Another limitation is the variability of immunohistochemistry, which was quantified to be 13.7% within batches. To limit this variability, 2 sections were taken for SEPT and LAT and the results were averaged. Additionally, for a given segment and protein, TIC and CTRL sections were stained in the same batch. Despite these limitations of short time course and variability in immunohistological analysis, significant results were found. Another limitation is that hemodynamic and leaflet length analyses were made comparing pre-TIC and TIC animals, whereas histological analyses compared TIC and CTRL animals. Whereas explanted pre-TIC tissue was not available to compare to explanted TIC tissue, the authors did verify that there were no significant differences between the annular and leaflet radiopaque marker

measurements of pre-TIC and CTRL animals. Another limitation was that animals were not randomized to groups. In addition, there were different numbers of animals in the TIC and CTRL groups, resulting in an unbalanced design. These numbers were caused by animal loss from the TIC group, most commonly caused by loss of the animal on anesthetic induction before the second set of marker and hemodynamic studies, because the animals were in florid heart failure. With respect to the lack of randomization, whereas each group displayed body weights and hemodynamics within a normal range, LV end systolic pressure of CTRL was found to be higher than TIC (P=0.004), whereas the CTRL animals weighed less (P=0.033); no difference was found between CTRL and pre-TIC with respect to LV end diastolic pressure or EF. The difference in LV end diastolic pressure between groups could be attributable to a number of factors, including level of anesthetic, loading, and adrenergic drive at the time of measurement. However, given that the CTRL group in this study was exclusively used for histological comparisons between valves, and that there was no comparison of absolute differences in tissue dimensions, the authors believe that this difference does not undermine our results.

Although the ovine MV has dynamics very similar to the human MV,[23,24] there are a number of anatomic differences, including less redundancy in the ovine MV leaflet,25,26 TIC may have subtle differences compared to DCM, although studies have shown that the hemodynamics14 and neurohormonal[15] changes elicited by TIC match those of human DCM. Lastly, the tantalum markers (total mass ≈20 mg) could have affected leaflet motion. However, studies have shown that even when enough markers are added to overload the ovine MV (total mass = 184 mg), MV motion does not change significantly.[3] Furthermore, these markers were present in both TIC and CTRL; therefore, they could not explain the differences found between TIC and CTRL. Finally, this study found a large number of correlations between MV structure, composition, and function, but further research will be required to determine causation, delineate the specific role of mitral regurgitation in the observed changes, and propose new therapeutic options.

Conclusion

This study shows that the MV leaflets are intimately and differentially involved in the DCM disease process, with changes in leaflet composition, structure, and valve cell phenotype. These results suggest that the MV leaflets themselves should be considered in DCM treatment strategies. Furthermore, the relationship between leaflet composition and changes in leaflet segment length suggest that changes in the extracellular matrix could be an underlying mechanism for the observed changes in leaflet motion, with the myofibroblast potentially playing an important role. The implicated link between altered leaflet strain and altered composition also reinforces the need to maintain physiological leaflet strains with appropriate annuloplasty design.

Acknowledgments

The authors thank all the members of the Grande-Allen laboratory, especially Indrajit Nandi.

Sources of Funding

Funding for this project came in part from Hertz Graduate Fellowship (EHS) and grants 5R01 HL067025-07 and 5R01 HL029589-25,

References

1. Kunzelman KS, Reimink MS, Cochran RP. Annular dilatation increases stress in the mitral valve and delays coaptation: a finite element computer model. Cardiovasc Surg 1997;5:427–434. [PubMed: 9350801]
2. He S, Lemmon JD Jr, Weston MW, Jensen MO, Levine RA, Yoganathan AP. Mitral valve compensation for annular dilatation: in vitro study into the mechanisms of functional mitral regurgitation with an adjustable annulus model. J Heart Valve Dis 1999;8:294–302. [PubMed: 10399664]
3. Timek TA, Lai DT, Dagum P, Liang D, Daughters GT, Ingels NB Jr, Miller DC. Mitral leaflet remodeling in dilated cardiomyopathy. Circulation 2006;114:I518–I523. [PubMed: 16820630]
4. Merryman WD, Youn I, Lukoff HD, Krueger PM, Guilak F, Hopkins RA, Sacks MS. Correlation between heart valve interstitial cell stiffness and transvalvular pressure: implications for collagen biosynthesis. Am J Physiol 2006;290:H224–H231.
5. Timek TA, Dagum P, Lai DT, Liang D, Daughters GT, Tibayan F, Ingels NB Jr, Miller DC. Tachycardia-induced cardiomyopathy in the ovine heart: mitral annular dynamic three-dimensional geometry. J Thorac Cardiovasc Surg 2003;125:315–324. [PubMed: 12579100]
6. Helmcke F, Nanda N, Hsiung M, Soto B, Adey C, Goyal R, Gatewood R Jr. Color Doppler assessment of mitral regurgitation with orthogonal planes. Circulation 1987;75:175–183. [PubMed: 3791603]
7. Montiel MM. Muscular apparatus of the mitral valve in man and its involvement in left-sided cardiac hypertrophy. Am J Cardiol 1970;26:341–344. [PubMed: 5474493]
8. Messier RH Jr, Bass BL, Aly HM, Jones JL, Domkowski PW, Wallace RB, Hopkins RA. Dual structural and functional phenotypes of the porcine aortic valve interstitial population: characteristics of the leaflet myofibroblast. J Surg Res 1994;57:1–21. [PubMed: 8041124]
9. Balachandran K, Konduri S, Sucosky P, Jo H, Yoganathan AP. An ex vivo study of the biological properties of porcine aortic valves in response to circumferential cyclic stretch. Ann Biomed Eng 2006;34:1655–1665. [PubMed: 17031600]
10. Vesely I, Noseworthy R. Micromechanics of the flbrosa and the ventricularis in aortic valve leaflets. J Biomech 1992;25:101–113. [PubMed: 1733978]
11. Stephens EH, Nguyen TC, Itoh A, Ingels NB Jr, Miller DC, Grande-Allen KJ. The effects of hemodynamics of regurgitation alone are sufficient for mitral valve leaflet remodeling. Circulation 2008;118:S243–S249. [PubMed: 18824762]
12. Schwammenthal E, Chen C, Benning F, Block M, Breithardt G, Levine RA. Dynamics of mitral regurgitant flow and orifice area: physiologic application of the proximal flow convergence method: clinical data and experimental testing. Circulation 1994;90:307–322. [PubMed: 8026013]
13. Willems I, Havenith M, Smits J, Daemen M. Structural alterations in heart valves during left ventricular pressure overload in the rat. Lab Invest 1994;71:127–133. [PubMed: 8041112]
14. Wilson JR, Douglas P, Hickey WF, Lanoce V, Ferraro N, Muhammad A, Reichek N. Experimental congestive heart failure produced by rapid ventricular pacing in the dog: cardiac effects. Circulation 1987;75:857–867. [PubMed: 3829344]
15. Riegger A, Liebau G. The renin-angiotensin-aldosterone system, antidiuretic hormone and sympathetic nerve activity in an experimental model of congestive heart failure in the dog. Clin Sci (Lond) 1982;62:465–469. [PubMed: 7075144]
16. Rabkin E, Aikawa M, Stone JR, Fukumoto Y, Libby P, Schoen FJ. Activated interstitial myofibroblasts express catabolic enzymes and mediate matrix remodeling in myxomatous heart valves. Circulation 2001;104:2525–2532. [PubMed: 11714645]
17. Chaput M, Handschumacher MD, Tournoux F, Hua L, Guerrero JL, Vlahakes GJ, Levine RA. Mitral leaflet adaptation to ventricular remodeling: occurrence and adequacy in patients with functional mitral regurgitation. Circulation 2008;118:845–852. [PubMed: 18678770]
18. Grande-Allen KJ, Borowski AG, Troughton RW, Houghtaling PL, Dipaola NR, Moravec CS, Vesely I, Griffin BP. Apparently normal mitral valves in patients with heart failure demonstrate biochemical and structural derangements: an extracellular matrix and echocardiographic study. J Am Coll Cardiol 2005;45:54–61. [PubMed: 15629373]

19. Gunja-Smith Z, Morales AR, Romanelli R, Woessner JF Jr. Remodeling of human myocardial collagen in idiopathic dilated cardiomyopathy. Role of metalloproteinases and pyridinoline cross-links. Am J Pathol 1996;148:1639–1648. [PubMed: 8623931]

20. Grande-Allen KJ, Barber JE, Klatka KM, Houghtaling PL, Vesely I, Moravec CS, McCarthy PM. Mitral valve stiffening in end-stage heart failure: evidence of an organic contribution to functional mitral regurgitation. J Thorac Cardiovasc Surg 2005;130:783–790. [PubMed: 16153929]

21. Kunzelman KS, Quick DW, Cochran RP. Altered collagen concentration in mitral valve leaflets: biochemical and finite element analysis. Ann Thorac Surg 1998;66:S198–S205. [PubMed: 9930448]

22. Kunzelman KS, Cochran RP, Murphree SS, Ring WS, Verrier ED, Eberhart RC. Differential collagen distribution in the mitral valve and its influence on biomechanical behaviour. J Heart Valve Dis 1993;2:236–244. [PubMed: 8261162]

23. Glasson JR, Komeda M, Daughters GT, Foppiano LE, Bolger AF, Tye TL, Ingels NB Jr, Miller DC. Most ovine mitral annular three-dimensional size reduction occurs before ventricular systole and is abolished with ventricular pacing. Circulation 1997;96:II-115–II-122.

24. Ormiston JA, Shah PM, Tel C, Wong M. Size and motion of the mitral valve annulus in man. II. Abnormalities in mitral valve prolapse. Circulation 1982;65:713–719. [PubMed: 7060250]

25. Brock R. The surgical and pathological anatomy of the mitral valve. Br Heart J 1952;14:489–513. [PubMed: 12987528]

26. Gorman JH III, Jackson BM, Gorman RC, Kelley ST, Gikakis N, Edmunds LH Jr. Papillary muscle discoordination rather than increased annular area facilitates mitral regurgitation after acute posterior myocardial infarction. Circulation 1997;96:II-124–II-127.

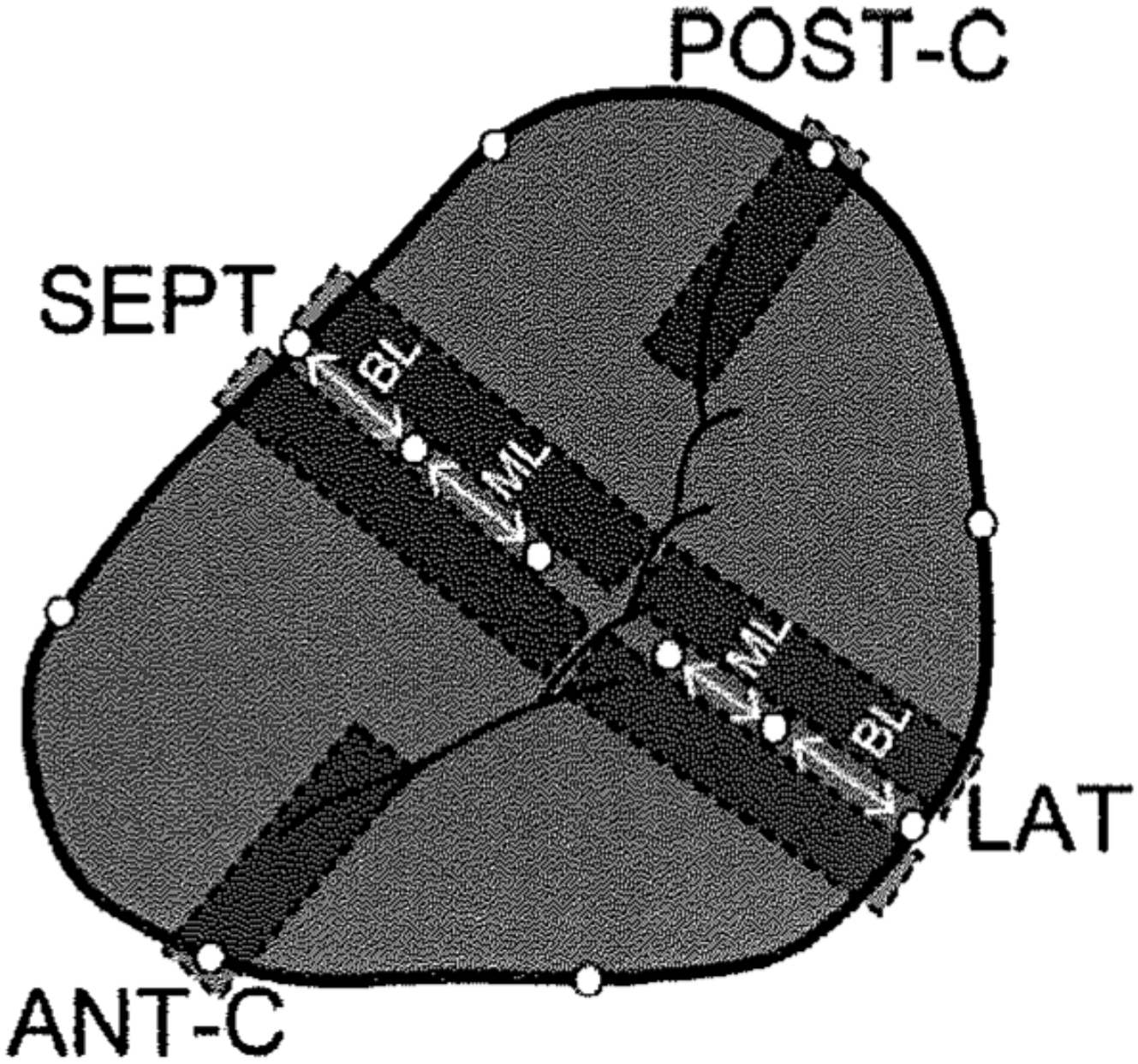

Figure 1.

Circles indicate the location of the implanted radiopaque markers. Gray rectangles indicate the locations from which tissue sections were taken (tissue sections were taken to either side of markers such that markers or their sutures were not included in the samples). In the case of septal segment (SEPT) and lateral segment (LAT), 2 tissue sections were analyzed and the results averaged. In the case of the anterior and posterior commissures (ANT-C, POST-C), 1 tissue section was taken from either side of the tantalum marker based on quality of the leaflet on each side. BL indicates basal leaflet, ML=mid-leaflet.

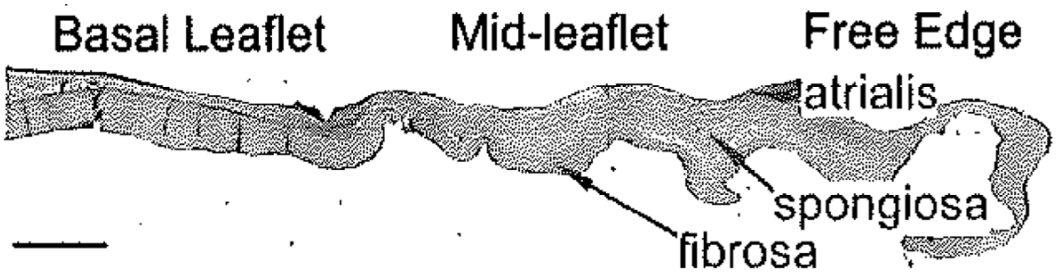

Figure 2.
Locations of leaflet regions and histological layers. Scale bar represents 2 mm.

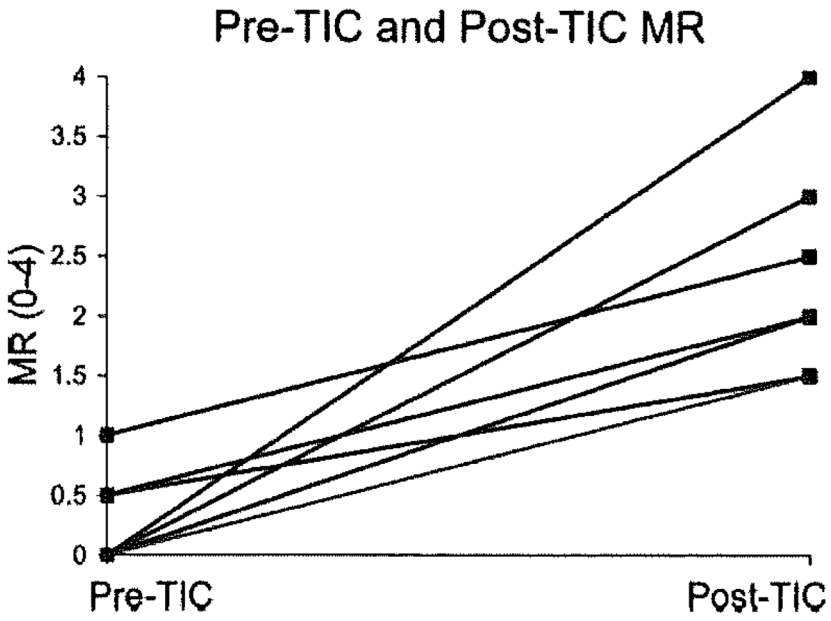

Figure 3.
Pre-TIC and post-TIC mitral regurgitation for each animal. Overall $P<0.0002$.

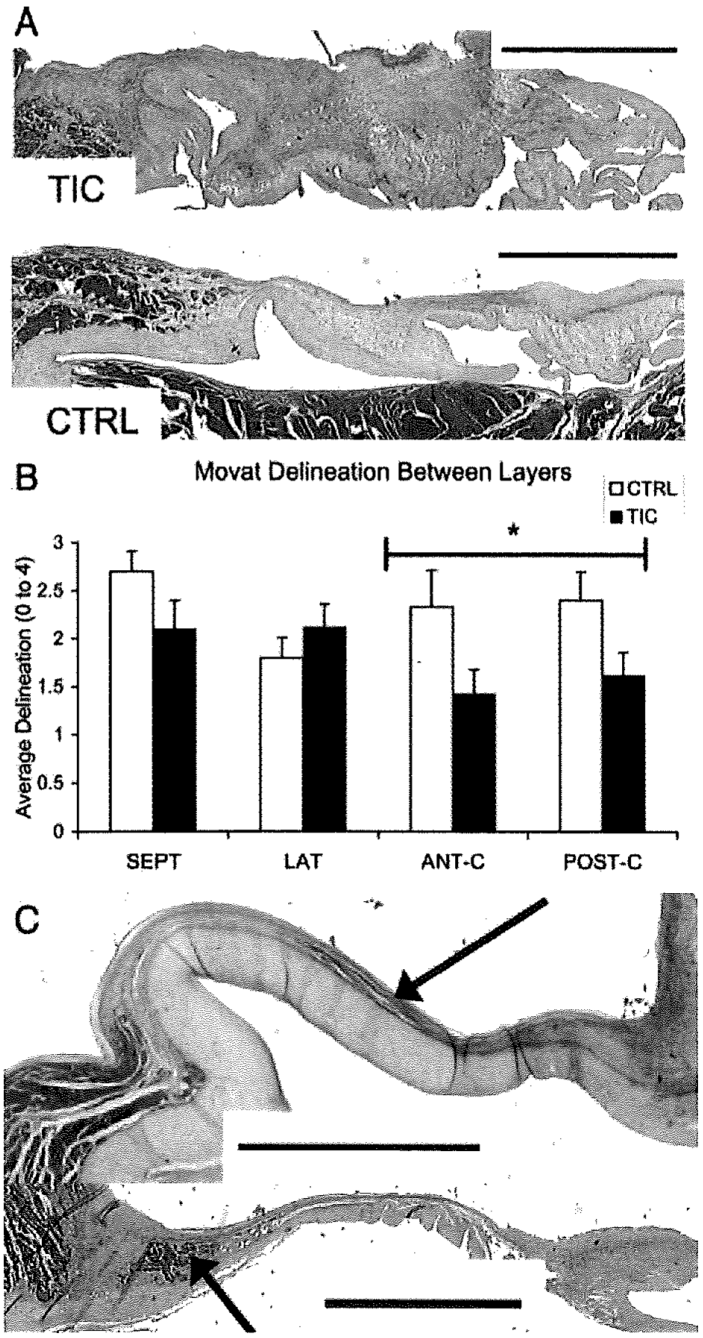

Figure 4.

A, Image illustrating the lack of delineation between layers in TIC (top) compared to CTRL (bottom). Samples are both LAT leaflets stained with Movat pentachrome and are oriented as in Figure 2. (green/blue=proteoglycans/glycosaminoglycans, yellow=collagen, red=muscle, black=elastic fibers). Scale bars represent 2 mm. B, Graph illustrating decrease in delineation in TIC compared to CTRL (P=0.014). *P=0.011. Error bars indicate the SEM. C, Examples of muscle found considerably more often in TIC compared to CTRL (9 TIC, 2 CTRL). Arrows point to muscle, which previous studies have shown to be atrial cardiac muscle.[7] Scale bars represent 2 mm and leaflets are oriented as in Figure 2.

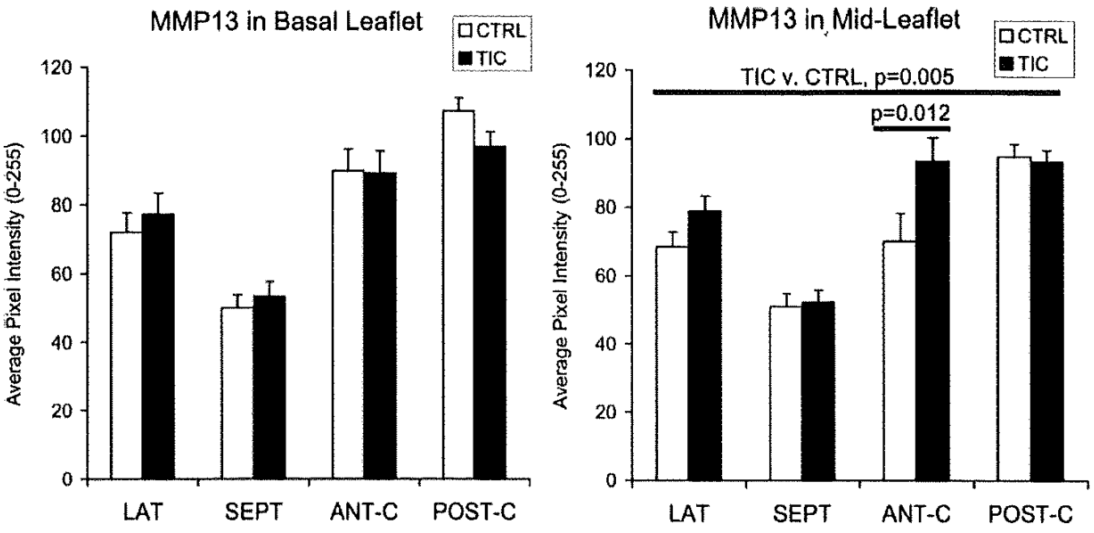

Figure 5.

MMP-13 in BL and ML of TIC and CTRL. In all Figures, the long horizontal line indicates the comparison between groups in the ANOVA, whereas the short horizontal line indicates results of the post hoc comparisons. Error bars indicate SEM.

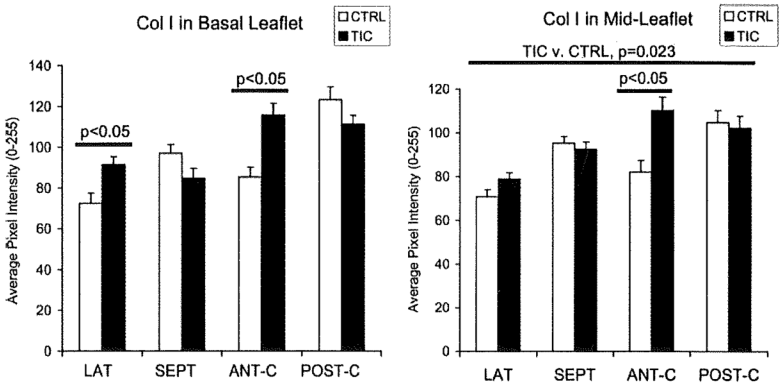

Figure 6.
Collagen **I** in BL and ML of TIC and CTRL. Error bars indicate SEM.

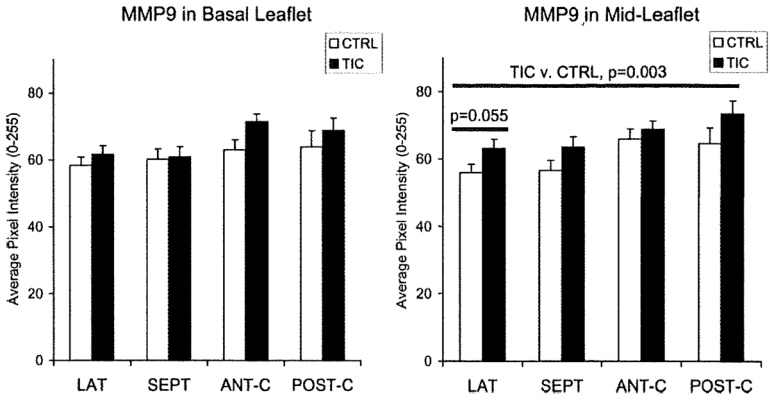

Figure 7.
MMP-9 in BL and ML of TIC and CTRL. Error bars indicate SEM.

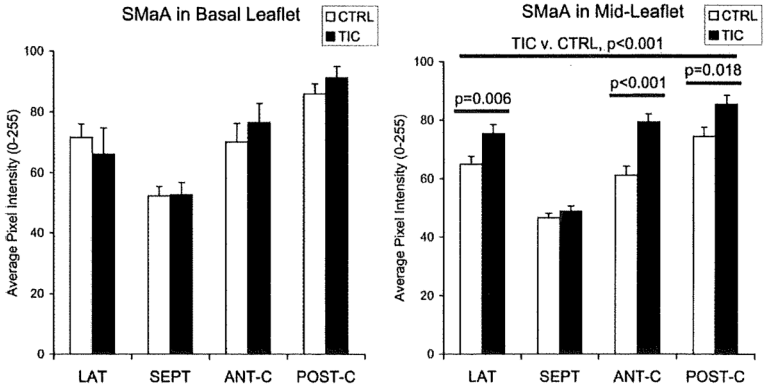

Figure 8.
SMaA in BL and ML of TIC and CTRL. Error bars indicate SEM.

Table 1

Panel of Antibodies Used in Immunohistochemistry

Protein	Function
Collagen turnover proteins	
Collagen I*	Predominant collagen in valve, provides tensile strength
Collagen III*	Reticular collagen
MMP-13†	Collagen degradation
Elastic fiber-related proteins	
Lysyl oxidase§	Involved in collagen and elastin cross-linking
Elastin¶	Predominant component of elastic fibers
MMP-9‡	Elastic fiber degradation
Proteoglycans and glycosaminoglycans	
Hyaluronan||	Glycosaminoglycan providing compressibility
Decorin*	Proteoglycan involved in collagen fibrillogenesis
Biglycan*	Proteoglycan involved in collagen fibrillogenesis
Valve cell activation	
SMaA**	Marker of an “activated” myofibroblast-like phenotype
NMM heavy chain††	Marker of an “activated” myofibroblast-like phenotype

*Gift from Dr Larry Fisher, NIH (Bethesda, Md).

†Chemicon (Temecula, Calif).

‡Assay Designs (Ann Arbor, Mich).

§Imgenex (San Diego, Calif).

¶Abcam (Cambridge, Mass).

||Associates of Cape Cod (Falmouth, Mass).

**Dakocytomation (Denmark).

††Covance (Berkeley, Calif).

Table 2

Pre-TIC and TIC Maximum Leaflet Segment Lengths

	Pre-TIC, cm	TIC, cm
Septal		
BL	1.17±0.21	1.22±0.15
ML	1.37±0.10	1.45±0.03*
Total Leaflet	2.49±0.10	2.65±0.15*
Lateral		
BL	0.63±0.20	0.66±0.20
ML	0.63±0.14	0.71±0.11*
Total leaflet	1.26±0.28	1.36±0.23*

* $P<0.05$ versus pre-TIC.

Data expressed as mean±SD.